Since January 2020 Elsevier has created a COVID-19 resource centre with free information in English and Mandarin on the novel coronavirus COVID-19. The COVID-19 resource centre is hosted on Elsevier Connect, the company's public news and information website.

Biochemical and Biophysical Research Communications 597 (2022) 30–36

Contents lists available at ScienceDirect

Biochemical and Biophysical Research Communications

journal homepage: www.elsevier.com/locate/ybbrc

The function of SARS-CoV-2 spike protein is impaired by disulfide-bond disruption with mutation at cysteine-488 and by thiol-reactive *N*-acetyl-cysteine and glutathione

Mana Murae [a, b, 1], Yoshimi Shimizu [b, c, 1], Yuichiro Yamamoto [a], Asuka Kobayashi [a], Masumi Houri [a], Tetsuya Inoue [a], Takuya Irie [a, b], Ryutaro Gemba [b], Yosuke Kondo [d], Yoshio Nakano [d], Satoru Miyazaki [d], Daisuke Yamada [e], Akiyoshi Saitoh [e], Isao Ishii [f], Taishi Onodera [g], Yoshimasa Takahashi [g], Takaji Wakita [h], Masayoshi Fukasawa [a, b, **], Kohji Noguchi [a, b, *]

[a] *Laboratory of Molecular Target Therapy, Faculty of Pharmaceutical Sciences, Tokyo University of Science, Yamasaki 2641, Noda, Chiba, 278-8510, Japan*
[b] *Department of Biochemistry and Cell Biology, National Institute of Infectious Diseases, 1-23-1, Toyama, Shinjuku-ku, Tokyo, 162-8640, Japan*
[c] *Department of Pharmaceutical Sciences, Teikyo Heisei University, 4-21-2 Nakano, Nakano-ku, 164-8530, Japan*
[d] *Department of Medical and Life Science, Faculty of Pharmaceutical Sciences, Tokyo University of Science, Yamasaki 2641, Noda, Chiba, 278-8510, Japan*
[e] *Laboratory of Pharmacology, Faculty of Pharmaceutical Sciences, Tokyo University of Science, Yamasaki 2641, Noda, Chiba, 278-8510, Japan*
[f] *Department of Health Chemistry, Showa Pharmaceutical University, Tokyo, 194-8543, Japan*
[g] *Research Center for Drug and Vaccine Development, National Institute of Infectious Diseases, 1-23-1, Toyama, Shinjuku-ku, Tokyo, 162-8640, Japan*
[h] *National Institute of Infectious Diseases, 1-23-1, Toyama, Shinjuku-ku, Tokyo, 162-8640, Japan*

ARTICLE INFO

Article history:
Received 18 January 2022
Accepted 26 January 2022
Available online 29 January 2022

Keywords:
SARS-CoV-2
Spike
Cysteine

ABSTRACT

Viral spike proteins play important roles in the viral entry process, facilitating attachment to cellular receptors and fusion of the viral envelope with the cell membrane. Severe acute respiratory syndrome coronavirus 2 (SARS-CoV-2) spike protein binds to the cellular receptor angiotensin converting enzyme-2 (ACE2) via its receptor-binding domain (RBD). The cysteine residue at position 488, consisting of a disulfide bridge with cysteine 480 is located in an important structural loop at ACE2-binding surface of RBD, and is highly conserved among SARS-related coronaviruses. We showed that the substitution of Cys-488 with alanine impaired pseudotyped SARS-CoV-2 infection, syncytium formation, and cell-cell fusion triggered by SARS-CoV-2 spike expression. Consistently, *in vitro* binding of RBD and ACE2, spike-mediated cell-cell fusion, and pseudotyped viral infection of VeroE6/TMPRSS2 cells were inhibited by the thiol-reactive compounds *N*-acetylcysteine (NAC) and a reduced form of glutathione (GSH). Furthermore, we demonstrated that the activity of variant spikes from the SARS-CoV-2 alpha and delta strains were also suppressed by NAC and GSH. Taken together, these data indicate that Cys-488 in spike RBD is required for SARS-CoV-2 spike functions and infectivity, and could be a target of anti-SARS-CoV-2 therapeutics.

1. Introduction

One of the four genera of the *Coronaviridae* family of viruses, beta-coronaviruses, is a positive-sense, single-stranded, enveloped RNA virus [1]. Severe acute respiratory syndrome coronavirus 2 (SARS-CoV-2) is the seventh identified member of the coronavirus family that is the causative agent of coronavirus disease 2019 (COVID-19) [2,3]. SARS-CoV-2 probably originates from Bats [4], and the SARS-CoV-2 cellular receptor in humans is angiotensin-converting enzyme 2 (ACE2) protein [5,6]. SARS-CoV-2 has been

* Corresponding author. Laboratory of Molecular Target Therapy, Faculty of Pharmaceutical Sciences, Tokyo University of Science, Yamasaki 2641, Noda, Chiba, 278-8510, Japan.
** Corresponding author. Department of Biochemistry and Cell Biology, National Institute of Infectious Diseases, 1-23-1, Toyama, Shinjuku-ku, Tokyo, 162-8640, Japan.
E-mail addresses: fuka@nih.go.jp (M. Fukasawa), noguchi-kj@rs.tus.ac.jp (K. Noguchi).
[1] These authors share equal first authorship.

https://doi.org/10.1016/j.bbrc.2022.01.106
0006-291X/

shown to infect various species whose ACE2s can bind to SARS-CoV-2 [7].

The D614G mutation was identified during the initial global pandemic period of COVID-19 as the dominant SARS-CoV-2 variant [8,9], and multiple variants have been reported since then. Based on recent updates by the WHO, four major types of variants of concern (VOCs) have been identified: alpha (first described in the United Kingdom), beta (first reported in South Africa), gamma (first reported in Brazil), and delta (first reported in India) [10]. These VOCs have distinctive mutations in the receptor binding domain (RBD) [11]. The delta variant is rapidly spreading worldwide [12], and elucidation of effective therapeutic targets for all mutants is desired.

The spike protein of SARS-CoV-2 is a key molecule for viral entry into host cells [13]. The conformational dynamics of the spike protein, especially at the RBD are required for its binding to the cellular receptor ACE2 [14]. The conformational flexibility and stability of viral proteins are affected by intramolecular and intermolecular disulfide bridges [15], and viral envelope protein-mediated virus attachment/cell membrane fusion is thought to depend on a thiol/disulfide balance within the viral surface complex [16,17]. Although the redox insensitivity of the SARS-CoV spike protein has been previously reported [18], the functional importance of the disulfide bridge in SARS-CoV and SARS-CoV-2 RBDs has been suggested using both computational and experimental approaches [19–22]. The disulfide bridge Cys-480-Cys-488 in RBD appears to contribute to the structural stability of the β-sheet loop motif [23,24], and discussed the possible therapeutic effects of thiol-based drugs on COVID-19 [19,25,26].

We demonstrated functional importance of Cys-488 in the SARS-CoV-2 spike protein in this study. We also showed the inhibitory effect of disulfide bridge-disrupting *N*-acetylcysteine (NAC) and a reduced form of glutathione (GSH) on the functional activity of RBDs from variant SARS-CoV-2. Our data suggest that the functional role of Cys-488 in the SARS-CoV-2 spike protein could be a good target for antiviral therapy.

2. Materials and methods

2.1. Cell and reagents

HEK293T, Vero (ATCC, CCL-81), and VeroE6/TMPRSS2 (JCRB, JCRB1819) cells were cultured in Dulbecco's modified Eagle's medium (DMEM) supplemented with 7.5% (v/v) fetal bovine serum (FBS) and kanamycin (50 μg/ml). Suspension-adapted FreeStyle 293-F (Thermo Fisher Scientific, R79007) cells were cultured in FreeStyle 293 Expression Medium (Thermo Fisher Scientific, Life Technologies Corp., Carlsbad, CA). FreeStyle 293-F cells were maintained in a spinner flask at 130 rpm using an orbital shaker at 37 °C in a humidified atmosphere of 8% CO_2. NAC and GSH were purchased from Sigma-Aldrich® (Merck KGaA, Darmstadt, Germany).

2.2. Pseudotyped SARS-CoV-2 preparation

The plasmid pUC57-2019-nCoV-S (Human), containing synthetic cDNA to express SARS-CoV-2 spike protein with human codon optimization was purchased from Genscript Japan Inc. (Tokyo, Japan), and cloned into the expression plasmid pcDNA3.1. Mutant spike cDNAs were further synthesized by GenScript. The plasmids used in this study are listed in Supplementary Table 1. For retrovirus-based pseudotyped virus production, 293T cells were co-transfected with spike-expressing plasmids containing the phCMV-Gag-Pol 5349 and reporter pTG-Luc126 plasmids [27] using the PEIpro® transfection reagent (Polyplus Transfection, New York, NY). Briefly, 2×10^6 293T cells were seeded in a T-25 flask one day before transfection, and the next day, the cells were co-transfected following the manufacturer's instructions. The next day, the growth medium was added to the flask for an additional 2 days of culture. The cell supernatant containing pseudotyped virus was collected, filtered through a 0.45 μm filter, and aliquoted to be stored at −80 °C.

2.3. Luciferase assay for pseudotyped virus infection

VeroE6/TMPRSS2 cells were seeded at $1–2 \times 10^4$/100 μL/well in a 96-well white plate. The next day, pseudotyped viruses were added to each well and cultured for three days. For thiol-reagent pretreatment, the virus was preincubated with glutathione or N-acetylcysteine-containing medium at the indicated concentrations for 30 min at 37 °C, and then added to the wells. After 3 days, the medium was removed. Cells were washed once with PBS and subsequently lysed using a luciferase assay reagent (PicaGene Meliora Star-LT Luminescence Reagent, TOYO B-NET Co., Ltd., Tokyo, Japan). Triplicate transduction was performed for each experiment. The average and SD were calculated, and the reproducibility was confirmed.

2.4. Immunofluorescence microscopic analysis

Cells were seeded at 10^4 cells/0.8 ml/well in poly D-lysin-coated 4-well slide chambers (Corning Inc., Corning, NY), and transfected the next day. After the indicated time, cells were fixed in 4% paraformaldehyde for 15 min, then permeabilized for 15 min with 0.2% Triton-X100 or Tween-20/PBS or not, and blocked with 1% BSA/PBS for 30 min. Cells were incubated with the primary antibody (0.5 μg/ml in 1% BSA/PBS) overnight at 4 °C, washed with PBS three times, and then subjected to secondary antibody treatment (× 1000–5000 dilution in 1% BSA/PBS). Fluorescence-conjugated secondary antibodies (goat anti-mouse IgG (H + L) cross-adsorbed Alexa Fluor® 488 and donkey anti-rabbit IgG (H + L) highly cross-adsorbed -Alexa Fluor® Plus 594) were purchased from Thermo Fisher Scientific (Life Technologies Corp., Carlsbad, CA). Antifade (Vectashield Vibrance Antifade Mounting Medium) for microscopic analysis was purchased from Vector Laboratories Inc. (Burlingame, CA, USA). Images were captured using a BZ-9000 microscope (KEYENCE, Osaka, Japan). For confocal analysis, a TCS SP8 confocal laser scanning microscope (Leica Microsystems GmbH, Wetzlar, Germany) and Leica Application Suite X Software (Leica) were used. Two-dimensional TIFF images were merged using Adobe® Photoshop CS4 Extended software (Adobe Systems Inc., San Jose, CA, USA).

2.5. Immunoblotting

Cells were lysed using an UltraRIPA buffer (BioDynamics Laboratory Inc., Tokyo, Japan). Proteins were resolved by SDS-PAGE and electrotransferred to an Immobilon-P membrane (EMD Millipore, Billerica, MA, USA). Western blotting was performed using the standard method, and the following primary antibodies were used. Anti-spike antibody (1A9) was purchased from GeneTex Inc. (Irvine, CA, USA). Secondary antibodies (anti-mouse IgG-HRP and anti-rabbit IgG-HRP) were purchased from Cytiva™ (Tokyo, Japan). Anti-glyceraldehyde 3-phosphate dehydrogenase (anti-GAPDH 3H12) was purchased from Medical & Biological Laboratories Co., Ltd. (Aichi, Japan). Horseradish peroxidase-conjugated donkey anti-rabbit IgG and horseradish peroxidase-conjugated sheep anti-mouse IgG (Amersham Biosciences Corp., Piscataway, NJ, USA) were used as secondary antibodies. Immunoblot signals were developed using the EzWestLumi plus® (ATTO Corp., Tokyo, Japan), and

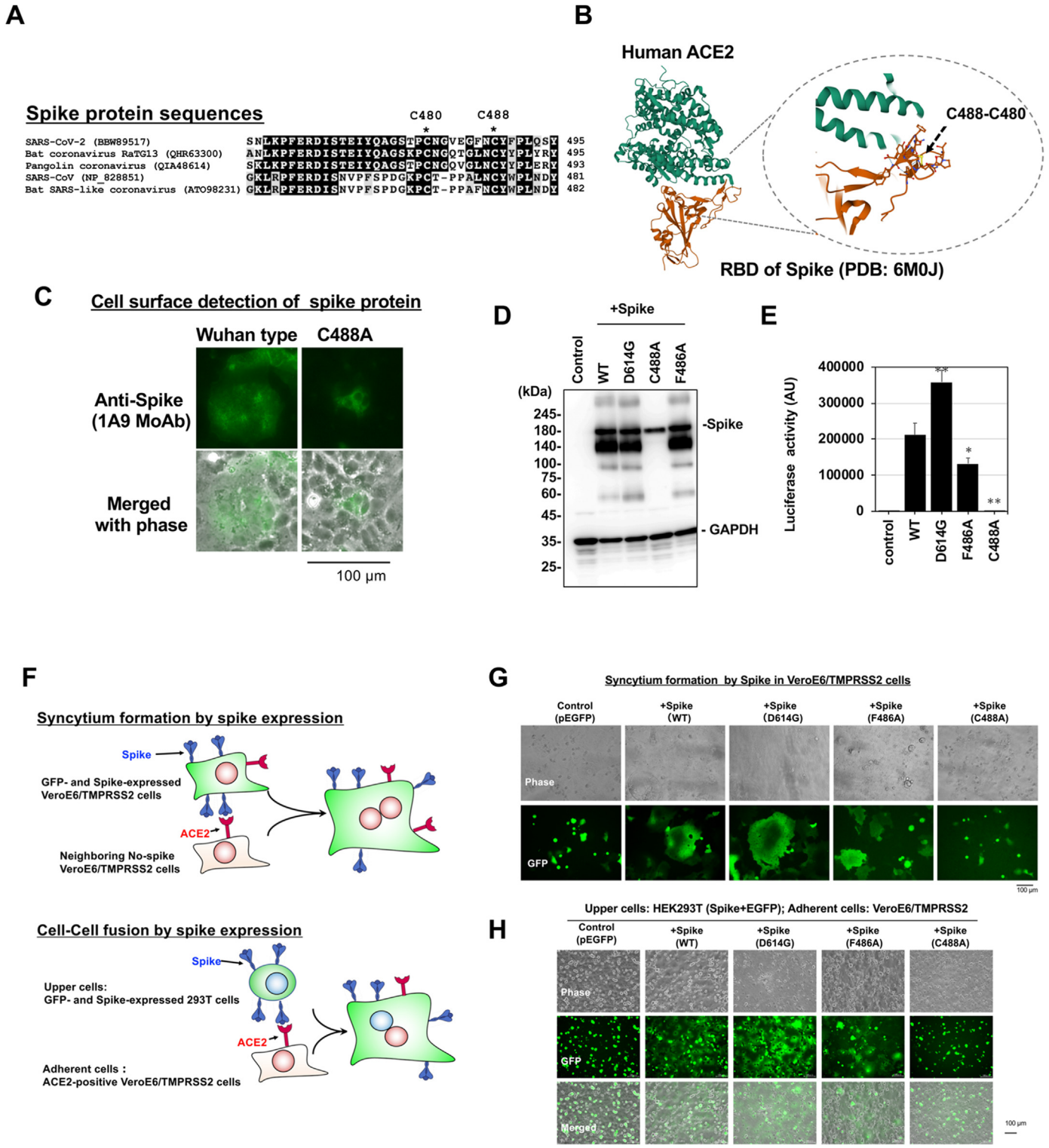

Fig. 1. The fusogenic and infective functions of the spike protein are disrupted by mutation of Cys-488.
(**A**) Amino acid sequence similarity around Cys-488 in SARS-CoV-2 RBD among ACE2-interactive spikes of SARS-related coronaviruses. The number at right position of each alignment is the amino acid position of the final Tyr (Y). (**B**) The structure model of ACE2 and RBD interaction from PDB. Disulfide bridges between Cys-480 and -488 are indicated.(**C**) C488A mutant spike expression did not induce syncytium formation. Expression of Wuhan type and C488A mutant spike proteins (Green signal) in Vero cells were probed in non-permeabilized cells. (**D**) Expression of mutant spike proteins detected by Western blot analysis Wuhan type (WT) and mutant spike proteins were expressed in 293T cells. GAPDH is shown as a loading control. (**E**) The infectivities of the pseudotyped viruses expressing each mutant spike protein were assessed by a reporter luciferase activities in VeroE6/TMPRSS2 cells. Luciferase activity is shown in arbitrary units (AU). Data from triplicated samples were expressed as the means ± standard deviation (SD). One-way ANOVA was performed to assess statistical significance. * indicates $p < 0.05$, and ** indicates $p < 0.01$. (**F**) The assays for spike-induced syncytium formation and cell-cell fusion were illustrated. (**G**) Syncytium formation by spike expression. Each mutant spike protein was co-expressed with GFP in VeroE6/TMPRSS2 cells. At 12 h after transfection, syncytium formation was visualized by green signal from GFP. Giant green cells indicate syncytium formation. (**H**) Spike-mediated cell-cell fusion. 293T cells transiently co-expressing each spike and GFP were overlaid on VeroE6/TMPRSS2 cells, and images of cell-cell fused giant adherent cells were captured after 3 h incubation. The lack of giant green adherent cells after treatment with the C488A mutant spike indicate a lack of cell-cell fusion between C488A mutant spike-expressing 293T cells and VeroE6/TMPRSS2 cells. Experiments were repeated independently twice and representative images are shown.

recorded with an ImageQuant LAS4000 mini image analyzer (GE Healthcare Japan Corp., Tokyo, Japan).

2.6. Recombinant RBD and soluble ACE2 preparation

The expression vector encoding the RBD of the Wuhan type SARS-CoV2 spike protein was constructed, as previously described [28]. The plasmids of the SARS-CoV-2 spike protein RBD mutants were prepared by site-directed mutagenesis using the KOD-Plus-Mutagenesis kit (Toyobo, Osaka, Japan). A gene encoding human soluble ACE2 (sACE2, GenBank accession number NM_001371415.1, residues 18–614 aa) fused to a C-terminal Fc tag was cloned into the pSecTag2 vector (Thermo Fisher Scientific) between Ig kappa signal peptide and stop codon. Recombinant proteins were produced using FreeStyle 293-F cells according to the manufacturer's instructions (Thermo Fisher Scientific). In brief, the supernatant from transfected cells was harvested on day 5 post-transfection, and supernatant fractions were separated by centrifugation at 9000×*g* for 10 min at room temperature. The supernatants were filtered through a 0.45 μm filter. The RBD peptides were purified with a HisTrap HP column (Cytiva), and the buffer was exchanged into PBS with Bio-Gel P6 Desalting Column (Bio-Rad Laboratories, Inc. CA, USA) using the Profinia protein purification system (Bio-Rad) according to the manufacturer's instructions. The human sACE2-Fc protein was purified using Ab-Capture Extra (ProteNova, Kagawa, Tokyo), and the buffer was replaced with PBS by gel filtration using a Sephadex G-25 column (PD-10, Cytiva). The concentrations of recombinant proteins were calculated by measuring the absorbance at 280 nm, with extinction coefficients of 1.55 $L \cdot g^{-1} \cdot cm^{-1}$ and 1.98 $L \cdot g^{-1} \cdot cm^{-1}$ for RBD and human sACE2-Fc, respectively.

2.7. ELISA for in vitro binding assay

EIA/RIA 96-well plates (Corning-Coaster, Tokyo, Japan) were coated with 200 μL of 250 ng/ml human sACE2-Fc protein overnight at 4 °C. Plates were washed with PBS containing 0.1% Tween 20 (PBS/Tween) and blocked with 200 μL of 5% BSA in PBS for 30 min at room temperature. SARS-CoV-2 RBD peptides (20 ng/well) were preincubated with 200 μL of 1% BSA in PBS (PBS/BSA) in the presence or absence of 10 mM GSH or NAC for 30 min at 37 °C, and then added to the wells. After incubation for 2h at room temperature, plates were washed with PBS/Tween and treated with 200 μL of PBS/BSA containing mouse Avi-tag monoclonal antibody (GenScript, Tokyo, Japan, A01738, 1:10,000 dilution) for 1.5 h at room temperature. After washing with PBS/Tween, the plates were further incubated with 200 μL of PBS/BSA containing HRP-conjugated anti-mouse IgG (1:5000 dilution, Jackson ImmunoResearch laboratory Inc., West Grove, PA, USA) for 1.5 h at room temperature. Bound RBD proteins were detected by the addition of 100 μL of 3,3′,5,5′-tetramethylbenzidine (TMB) substrate, 1-Step™ Ultra TMB-ELISA Substrate Solution (Thermo Fisher Scientific). The plates were then incubated for 5–10 min and the color change was monitored visually. The reaction was stopped by the addition of 50 μL of 2 M H_2SO_4. The optical density was measured at 450 nm using an iMark microplate reader (Bio-Rad).

2.8. Statistical analysis

In vitro experiments were repeated independently at least twice, and similar results were obtained. Quantitative results are presented as mean ± SD (n = 3) from triplicate samples. Student's *t*-test or one-way ANOVA was used to evaluate the significance of

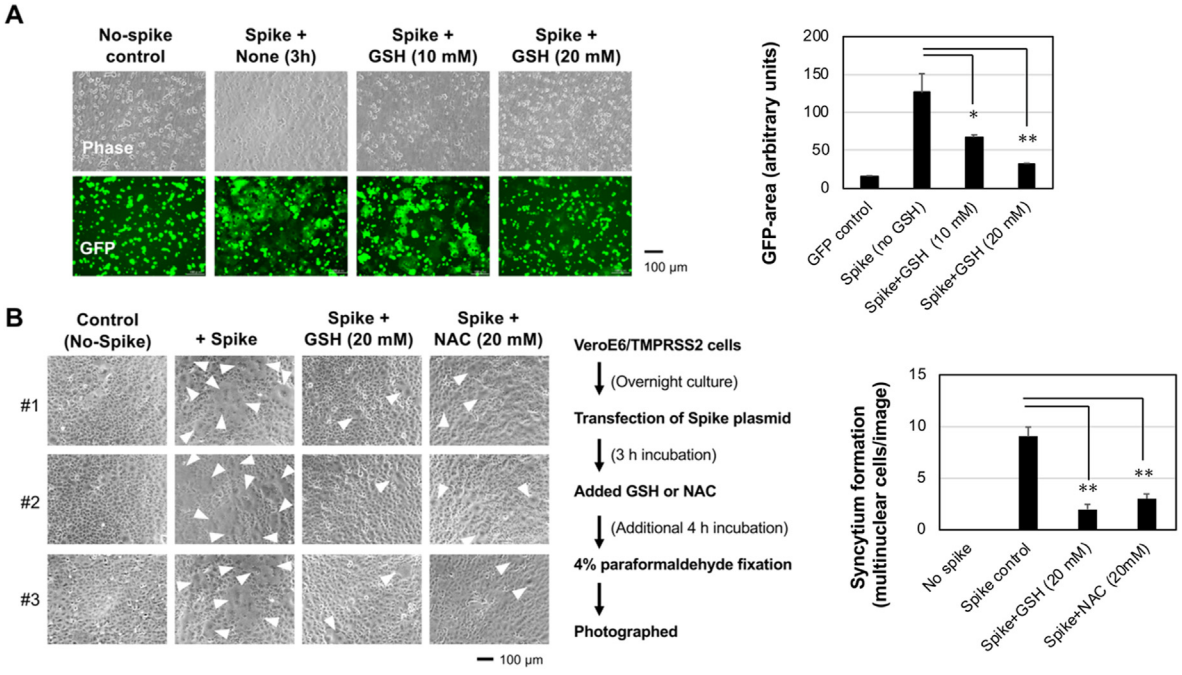

Fig. 2. NAC and GSH impaired spike-mediated cell-cell fusion and syncytium formation.
(**A**) Spike-expressing 293T cells were overlaid on VeroE6/TMPRSS2 cells in the presence of GSH for 3 h at the indicated doses. Cell-cell fusion, recognized as the generation of adherent green cells, was suppressed by 20 mM GSH treatment.(**B**) Spike-induced syncytium formation was inhibited by thiol-reactive GSH and NAC. The inhibition protocol is shown at bottom. Three independent field images are shown (#1–3). White arrowheads indicate giant syncytium cells. Experiments were repeated independently twice and representative images are shown. GFP-positive area/image (A) or syncytium multinuclear cells (B) were quantified with ImageJ software, and results from three images were expressed as the means ± standard SD (Right graphs). One-way ANOVA was performed to assess statistical significance. * indicates $p < 0.05$, and ** indicates $p < 0.01$.

differences between the experimental groups and the control group with similar variances. Differences were considered statistically significant at $p < 0.05$.

3. Results

3.1. Cys-488 is essential for the fusogenic activity by the spike protein

The spike protein of SARS-CoV-2 exerts cellular membrane fusogenic activity to facilitate viral entry via RBD binding to ACE2 [29,30]. Cys-488, which forms a disulfide bridge in the SARS-CoV-2 spike protein, is a conserved residue in SARS-related viruses located at the surface of the RBD-ACE2 interaction (Fig. 1A and B), and C488A spike mutant, in which the Cys-488 was substituted with alanine, did not induce syncytium formation (Fig. 1C). Other spike expressions of the Wuhan-type, D614G, F486A, and C488A mutant were confirmed (Fig. 1D), and the pseudotyped virus infection assay showed that the C488A mutant pseudotyped virus lost apparent infectious activity (Fig. 1E).

Fusogenic activities of these mutant spike proteins were also assessed by syncytium formation and cell-cell fusion assays (Fig. 1F). Microscopic analysis showed that C488A mutant spike lost syncytium formation and cell-cell fusion activities (Fig. 1G and H, respectively). Since the disulfide bridge between Cys-488 and Cys-480 is critical for ACE2-interacting loop structure [22], mutation at Cys-488 might disrupt structural stability around ACE2-interacting loop essential for spike function.

3.2. Thiol-reactive NAC and GSH suppressed spike-mediated syncytium formation and cell-cell fusion

To examine the sensitivity of the disulfide bridge for ACE2-binding activity of spike protein against thiol-reactive agents, the cell-cell fusion between spike-expressing 293T cells and ACE2-expressing VeroE6/TMPRSS2 cells was tested after pretreatment with the thiol-reactive reducing agent GSH. The spike-mediated cell-cell fusion was suppressed by GSH in a dose-dependent manner (Fig. 2A), and spike-induced syncytium formation, another hallmark of the fusogenic activity of the spike protein, was also reduced by GSH and related NAC treatment in VeroE6/TMPRSS2 cells (Fig. 2B). Therefore, the spike functions were sensitive to the thiol-reactive agents.

3.3. Thiol-reactive NAC and GSH inhibited pseudotyped SARS-CoV-2 infectivity

Wuhan-type spike-expressing pseudotyped virus infection in VeroE6/TMPRSS2 cells was decreased by NAC and GSH treatment in a dose-dependent manner (Fig. 3A). Both thiol-reactive agents also showed inhibitory activity against other variant spike-mediated pseudotyped virus infection (Fig. 3B). In our cell culture condition, NAC and GSH at indicated concentration did not show any cytotoxicity. These observations suggested that the disulfide bridge(s) in the spike protein of the widely spreading variant SARS-CoV-2 alpha and delta would be sensitive to thiol-reactive agents such as the early Wuhan-type spike protein.

3.4. Thiol-reactive NAC and GSH suppressed in vitro binding of variants spike RBD to ACE2

The effects of NAC and GSH on the *in vitro* binding between RBD of SARS-CoV-2 spike protein and ACE2 were tested. We observed that NAC and GSH inhibited the binding between RBD and ACE2 in a dose-dependent manner (Fig. 4A). Next, *in vitro* binding assay

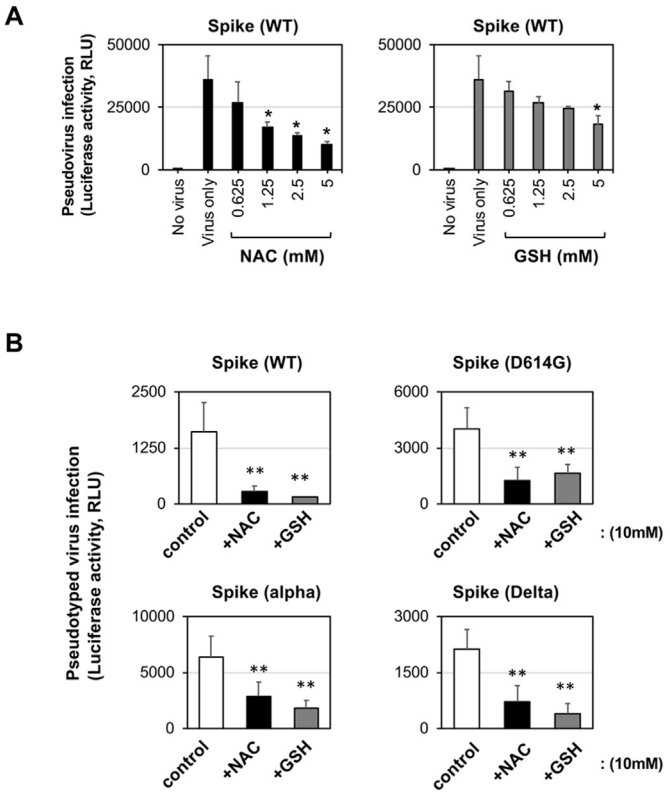

Fig. 3. NAC and GSH impaired pseudotyped SARS-CoV-2 infection
(**A**) Dose-dependent inhibition of Wuhan-type (WT) spike-expressing pseudotyped SARS-CoV-2 infection by NAC and GSH in VeroE6/TMPRSS2 cells.(**B**) Inhibition of variant spike-expressing pseudotyped SARS-CoV-2 infectivity by NAC and GSH in VeroE6/TMPRSS2 cells. Experiments were repeated independently twice and similar results were observed. Data from triplicated samples were expressed as the means ± standard SD. One-way ANOVA was performed to assess statistical significance. * indicates $p < 0.05$, and ** indicates $p < 0.01$.

showed that both NAC and GSH inhibited the ACE2-binding activity of all the tested variant RBDs; the alpha, beta, gamma, and delta types (Fig. 4B and C). These data indicate that the RBDs of the variant SARS-CoV-2 spike protein are sensitivities to thiol-reactive agents. Collectively, these data are consistent with the weakness of the spike protein against thiol-reactive agents.

4. Discussion

The binding of the SARS-CoV-2 spike protein to its cellular receptor ACE2 is the first step in viral cell entry and infection [31]. An intramolecular disulfide bridge of the spike protein between Cys-488 and Cys-480 in its RBD is located at the ACE2-binding surface and thought to be important for the molecular structure to bind ACE2 [6,14,23,24,32]. Here, we showed that the C488A spike mutant lost its fusogenic and infectious activities. The thiol-reactive agents NAC and GSH suppressed both spike-induced cellular fusogenic activity and pseudotyped viruses infection. These two thiol-reactive agents also suppressed the *in vitro* ACE2-binding ability of several RBDs with current epidemic variant strains, alpha-, beta-, gamma-, and delta-type. Collectively, the binding between spike and ACE2 is sensitive to the thiol-reactive reducing agent, and the disulfide bridge at Cys-488 would have a significant role in the binding of RBD to ACE2.

The impact of the disulfide bridge in the SARS-CoV-2 spike protein on the ACE2-binding activity of the RBD has been suggested in prior computational studies [20,33]. However, the functional

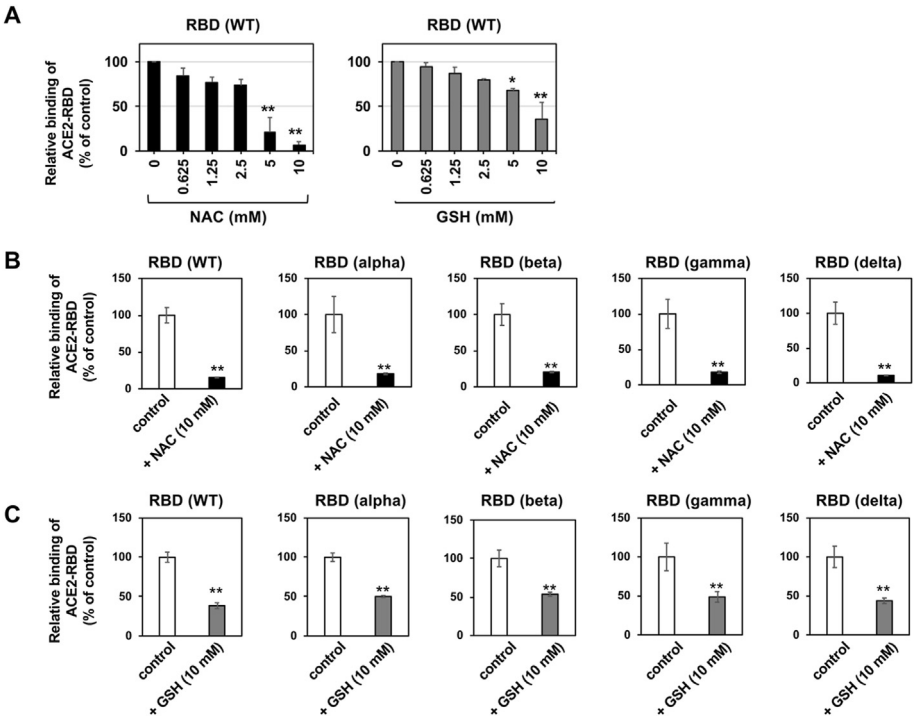

Fig. 4. NAC and GSH impaired variant RBD binding to ACE2 *in vitro*.
(**A**) Dose-dependent inhibition of Wuhan-type recombinant RBD proteins binding to ACE2 by NAC and GSH.(**B**) ACE2-binding activity of variants RBD protein was inhibited by NAC. (**C**) ACE2-binding activity of variants RBD protein was inhibited by GSH.Above experiments were repeated independently twice and similar results were observed. Data from triplicated samples were expressed as the means ± SD. Student's *t*-test was performed to assess statistical significance. ** indicates $p < 0.01$.

impact of only one disulfide bridge in SARS-CoV-2 spike protein remains to be determined [20]. Star et al. performed deep mutational analysis of RBD using a yeast display system, suggesting possible impact of Cys-488 mutations on the ACE2-binding ability [34]. The possible therapeutic efficacy of NAC on COVID-19 has been suggested [26], and the most recent papers by Manček-Keber et al. and Grishin et al. consistently reported that thiol-reactive compounds would target spike protein, and disruptions of Cys-480 and Cys-488 diminish the fusogenic activity of the SARS-CoV-2 spike [21,22]. Additionally, our independent study here showed that RBD-ACE2 binding-mediated functions of variant spike proteins were directly suppressed by thiol-reactive agents. Therefore, the results of this and other studies support the idea that thiol-reactive, disulfide bridge-targeting compounds would be effective against various SARS-CoV-2 variants. However, it should be careful that Cys-488 is not a selective target for NAC and GSH, and other disulfide bridges might be also affected by these agents. As Cys-488 selective compound is not discovered, and much effort and compound screening would be required for looking for unique compound targeting the Cys488-Cys-480 loop structure in the future.

Contributions

Conceptualization, M.F. and K.N.; Investigation, M.M., Y.S., Y.Y., M.F., and K.N.; Resources, A.K., M.H., T.I., T.I., R.G., Y.K., Y.N., S.M., D.Y., A.S., T.O., Y.Y., and T.W.; writing-original draft preparation, M.M., Y.S., M.F., and K.N.; writing-review and editing, M.M., Y.Y., I. I., M.F., and K.N.; Funding acquisition, M.F. and K.N. All authors have read and agreed to the published version of the manuscript.

Funding

This work was supported by an on-campus grant in TUS, funded by donations from “Account for Donations to Develop Vaccine and Medicine to Treat COVID-19” established by the Sumitomo Mitsui Trust Bank, Limited, and research grants from the Japan Agency for Medical Research and Development(AMED), Japan Program for Infectious Diseases Research and Infrastructure (Interdisciplinary Cutting-edge Research) [Grant No. 21wm0325032j0201 to MF].

Declaration of interest

☒ The authors declare that they have no known competing financial interests or personal relationships that could have appeared to influence the work reported in this paper.

☐ The authors declare the following financial interests/personal relationships which may be considered as potential competing interests:

Acknowledgments

We thank all the members of our laboratory for their technical support.

Appendix A. Supplementary data

Supplementary data to this article can be found online at https://doi.org/10.1016/j.bbrc.2022.01.106.

References

[1] P.C.Y. Woo, Y. Huang, S.K.P. Lau, K.Y. Yuen, Coronavirus genomics and bioinformatics analysis, Viruses 2 (2010) 1805–1820, https://doi.org/10.3390/v2081803.

[2] A.E. Gorbalenya, S.C. Baker, R.S. Baric, et al., The species Severe acute respiratory syndrome-related coronavirus: classifying 2019-nCoV and naming it SARS-CoV-2, Nat. Microbiol. 5 (2020) 536–544, https://doi.org/10.1038/s41564-020-0695-z.

[3] N. Zhu, D. Zhang, W. Wang, et al., A novel coronavirus from patients with pneumonia in China, 2019, N. Engl. J. Med. 382 (2020) 727–733, https://doi.org/10.1056/nejmoa2001017.
[4] P. Zhou, X. lou Yang, X.G. Wang, et al., A pneumonia outbreak associated with a new coronavirus of probable bat origin, Nature 579 (2020) 270–273, https://doi.org/10.1038/s41586-020-2012-7.
[5] M. Letko, A. Marzi, V. Munster, Functional assessment of cell entry and receptor usage for SARS-CoV-2 and other lineage B betacoronaviruses, Nat. Microbiol. 5 (2020) 562–569, https://doi.org/10.1038/s41564-020-0688-y.
[6] Q. Wang, Y. Zhang, L. Wu, et al., Structural and functional basis of SARS-CoV-2 entry by using human ACE2, Cell 181 (2020) 894–904, https://doi.org/10.1016/j.cell.2020.03.045, e9.
[7] L. Wu, Q. Chen, K. Liu, et al., Broad host range of SARS-CoV-2 and the molecular basis for SARS-CoV-2 binding to cat ACE2, Cell Discov. 6 (2020), https://doi.org/10.1038/s41421-020-00210-9.
[8] B. Korber, W.M. Fischer, S. Gnanakaran, et al., Tracking changes in SARS-CoV-2 spike: evidence that D614G increases infectivity of the COVID-19 virus, Cell 182 (2020) 812–827, https://doi.org/10.1016/j.cell.2020.06.043, e19.
[9] E. Volz, V. Hill, J.T. McCrone, et al., Evaluating the effects of SARS-CoV-2 spike mutation D614G on transmissibility and pathogenicity, Cell 184 (2021) 64–75, https://doi.org/10.1016/j.cell.2020.11.020, e11.
[10] F. Konings, M.D. Perkins, J.H. Kuhn, et al., SARS-CoV-2 Variants of Interest and Concern naming scheme conducive for global discourse, Nat. Microbiol. 6 (2021) 821–823, https://doi.org/10.1038/s41564-021-00932-w.
[11] J.A. Plante, B.M. Mitchell, K.S. Plante, et al., The variant gambit: COVID-19's next move, Cell Host Microbe 29 (2021) 508–515, https://doi.org/10.1016/j.chom.2021.02.020.
[12] Vaidyanathan G., Coronavirus Variants Are Spreading in India — what Scientists Know So Far, (n.d.).
[13] F. Li, Structure, function, and evolution of coronavirus spike proteins, Annu. Rev. Virol. 3 (2016) 237–261, https://doi.org/10.1146/annurev-virology-110615-042301.
[14] D. Wrapp, N. Wang, K.S. Corbett, et al., Cryo-EM Structure of the 2019-nCoV Spike in the Prefusion Conformation, 2019. http://science.sciencemag.org/.
[15] M. McCallum, A.C. Walls, J.E. Bowen, et al., Structure-guided covalent stabilization of coronavirus spike glycoprotein trimers in the closed conformation, Nat. Struct. Mol. Biol. 27 (2020) 942–949, https://doi.org/10.1038/s41594-020-0483-8.
[16] H. J-p Ryser, E.M. LEVYt, R. Mandel, G.J. DISCIULLOt, Inhibition of human immunodeficiency virus infection by agents that interfere with thiol-disulfi'de interchange upon virus-receptor interaction, 1994.
[17] T.M. Gallagher, Murine Coronavirus Membrane Fusion Is Blocked by Modification of Thiols Buried within the Spike Protein, 1996. https://journals.asm.org/journal/jvi.
[18] D. Lavillette, R. Barbouche, Y. Yao, et al., Significant redox insensitivity of the functions of the SARS-CoV spike glycoprotein: comparison with HIV envelope, J. Biol. Chem. 281 (2006) 9200–9204, https://doi.org/10.1074/jbc.M512529200.
[19] D. Giustarini, A. Santucci, D. Bartolini, F. Galli, R. Rossi, The age-dependent decline of the extracellular thiol-disulfide balance and its role in SARS-CoV-2 infection, Redox Biol. 41 (2021), https://doi.org/10.1016/j.redox.2021.101902.
[20] S. Hati, S. Bhattacharyya, Impact of thiol-disulfide balance on the binding of covid-19 spike protein with angiotensin-converting enzyme 2 receptor, ACS Omega 5 (2020) 16292–16298, https://doi.org/10.1021/acsomega.0c02125.
[21] M. Manček-Keber, I. Hafner-Bratkovič, D. Lainšček, et al., Disruption of disulfides within RBD of SARS-CoV-2 spike protein prevents fusion and represents a target for viral entry inhibition by registered drugs, FASEB (Fed. Am. Soc. Exp. Biol.) J. 35 (2021), https://doi.org/10.1096/fj.202100560R.
[22] A.M. Grishin, N.v. Dolgova, S. Landreth, et al., Disulfide bonds play a critical role in the structure and function of the receptor-binding domain of the SARS-CoV-2 spike antigen, J. Mol. Biol. 434 (2022), https://doi.org/10.1016/j.jmb.2021.167357.
[23] P. Baral, N. Bhattarai, M.L. Hossen, et al., Mutation-induced changes in the receptor-binding interface of the SARS-CoV-2 Delta variant B.1.617.2 and implications for immune evasion, Biochem. Biophys. Res. Commun. 574 (2021) 14–19, https://doi.org/10.1016/j.bbrc.2021.08.036.
[24] L. Guruprasad, Evolutionary relationships and sequence-structure determinants in human SARS coronavirus-2 spike proteins for host receptor recognition, Proteins: Struct. Funct. Bioinf. 88 (2020) 1387–1393, https://doi.org/10.1002/prot.25967.
[25] F. Silvagno, A. Vernone, G.P. Pescarmona, The role of glutathione in protecting against the severe inflammatory response triggered by covid-19, Antioxidants 9 (2020) 1–16, https://doi.org/10.3390/antiox9070624.
[26] H. Ibrahim, A. Perl, D. Smith, et al., Therapeutic blockade of inflammation in severe COVID-19 infection with intravenous N-acetylcysteine, Clin. Immunol. 219 (2020), https://doi.org/10.1016/j.clim.2020.108544.
[27] S. Rafique, M. Idrees, A. Ali, K.I. Sahibzada, M. Iqbal, Generation of infectious HCV pseudo typed particles and its utilization for studying the role of CD81 & SRBI receptors in HCV infection, Mol. Biol. Rep. 41 (2014) 3813–3819, https://doi.org/10.1007/s11033-014-3247-x.
[28] S. Moriyama, Y. Adachi, T. Sato, et al., Temporal maturation of neutralizing antibodies in COVID-19 convalescent individuals improves potency and breadth to circulating SARS-CoV-2 variants, Immunity 54 (2021) 1841–1852, https://doi.org/10.1016/j.immuni.2021.06.015, e4.
[29] Y. Cai, J. Zhang, T. Xiao, et al., Distinct Conformational States of SARS-CoV-2 Spike Protein, 2020. https://www.science.org.
[30] J. Buchrieser, J. Dufloo, M. Hubert, et al., Syncytia formation by SARS-CoV-2-infected cells, EMBO J. 39 (2020), https://doi.org/10.15252/embj.2020106267.
[31] C.B. Jackson, M. Farzan, B. Chen, H. Choe, Mechanisms of SARS-CoV-2 entry into cells, Nat. Rev. Mol. Cell Biol. (2021), https://doi.org/10.1038/s41580-021-00418-x.
[32] J. Lan, J. Ge, J. Yu, et al., Structure of the SARS-CoV-2 spike receptor-binding domain bound to the ACE2 receptor, Nature 581 (2020) 215–220, https://doi.org/10.1038/s41586-020-2180-5.
[33] T. Meirson, D. Bomze, G. Markel, Structural basis of SARS-CoV-2 spike protein induced by ACE2, Bioinformatics 37 (2021) 929–936, https://doi.org/10.1093/bioinformatics/btaa744.
[34] T.N. Starr, A.J. Greaney, S.K. Hilton, et al., Deep mutational scanning of SARS-CoV-2 receptor binding domain reveals constraints on folding and ACE2 binding, Cell 182 (2020) 1295–1310, https://doi.org/10.1016/j.cell.2020.08.012, e20.